Research Report

Mechanical Properties and Solder Joint Reliability of Low-Melting Sn-Bi-Cu Lead Free Solder Alloy

Hisaaki Takao, Akira Yamada, Hideo Hasegawa

低温系Sn-Bi-Cu鉛フリーはんだの機械的特性および接合信頼性

髙尾尚史，山田明，長谷川英雄

Abstract

The influence of alloy composition of low-melting Sn-Bi-Cu lead-free solder alloys on mechanical properties and solder joint reliabilities were investigated. The mechanically optimum alloy composition is Sn-40Bi-0.1Cu (mass%). The addition of 40mass%Bi improves the ductility and restrains the fillet-lifting, which are problems of lead-free solders with Bi. The addition of copper improves both the ductility and Cu leaching resistance of Sn-40Bi. The joint strength and thermal fatigue resistance of the Sn-40Bi-0.1Cu solder joints are superior to those of Sn-37Pb.

Keywords Lead-free, Tensile strength, Elongation, Shear strength, Thermal fatigue, Super plasticity

要　旨

本研究では，電子部品への熱的損傷が低減できる低温系Sn-Bi-Cu系合金に着目し，機械的特性および接合信頼性に及ぼす合金組成の影響について検討した。Bi含有量が40mass%付近のSn-BiおよびSn-Bi-Cu系合金は超塑性的な挙動を示し，最適組成であるSn-40Bi-0.1Cuの伸びは25°Cで171%，80°Cで516%に達し，従来のSn-37Pbの2.5倍以上の延性を有することがわかった。この超塑性的な挙動は合金組織と密接に関係しており，初晶Snとそれを網目状に取り囲むSn-Bi共晶あるいはSn-Bi-Cu共晶領域ですべりが生じることにより発現したと考えられる。Sn-40Bi-0.1Cuによるはんだ接合部の接合強度，耐熱疲労特性および耐Cu食われ性は現行のSn-37Pbはんだよりも優れており，信頼性の高い接合部が得られることを実証した。

キーワード　鉛フリー，引張強度，伸び，接合強度，熱疲労，超塑性

1. Introduction

For global environment conservation, many active researches on replacing the conventional Sn-Pb eutectic solder with a Pb-free solder have been carried out. In Europe, the use of lead will be banned after July 2007.[1-3] In Japan, replacement of Pb-free solder for Sn-Pb solder has been inescapably carried on by amendment of the regulations in the Waste Disposal Law and the implementation of the Electric Appliance Recycling Law.

Among lead-free solder materials, Sn-Ag alloys appear to be promising substitutes due to their high joint reliability. However, Sn-Ag alloys are not easily applied to some electronic components which have low-heat-tolerance because of the high melting temperature of these alloys.

As another alternative, lead-free solders containing Bi offer a low-melting temperature, which enable a lower soldering temperature, and have high tensile strength. These advantages have attracted a great deal of attention to lead-free solders containing Bi. Adding Bi to the alloy, however, makes the solder less ductile,[4] making it difficult to alleviate the thermal stress and strain in the joints. In addition, a joint defect called fillet lifting[5] occurring in the flow-soldering process has been a serious problem of these alloys on the joint reliability.

In this paper, we describe the improvement of the mechanical properties and joint reliability focusing on low-melting Sn-Bi alloys.[6]

2. Experimental

2. 1 Mechanical properties

The ultimate tensile strength and rapture elongation of the Sn-Bi alloys (Bi content: 0-62 mass% (hereinafter denoted as %)) were evaluated by tensile test.

Figure 1 shows the shape of the specimens used in the tensile test. Three pieces of specimens were machined from a cast ingot ($20\times15\times60$ mm^3). The specimens were annealed at 50^{o}C for 24h to remove the stress and strain induced by the machining. The specimens were also tested after aging for a week or longer at 25^{o}C. The tensile tests were conducted three times each at the strain rate of 1×10^{-2} to 1×10^{-4}s^{-1} at 25^{o}C and 80^{o}C.

2. 2 Joint reliability

Joint reliability was evaluated by a shear strength test and a thermal fatigue test of solder joints. In the shear test, the shear strength of lap-joint specimen was measured using Cu plates as shown in **Fig. 2**. After the surface of the Cu plates was electrolytically polished, the joining area (3×3mm^2) was pretinned with a solder. The two plates were soldered to each other at 230^{o}C, and the thickness of solder joint was controlled to be 100μm. The shear tests was conducted three times each at the strain rate of 3×10^{-3}s^{-1} at 25^{o}C and 80^{o}C. In addition, the specimens were heated at 80^{o}C for 1000h to examine the influence of the heat treatment on the joint strength.

In the thermal fatigue test, the thermal fatigue resistance of the solder joint was evaluated by a thermal cycling test. Samples were prepared, using a reflow-soldering technique with sheet solder on a hot plate, by joining a ceramic chip resistor (dimensions: $4.5\times3.2\times0.6$mm^3, surface finish of electrode: 95Sn-5Pb, number of pieces mounted on a board: 5) to an FR-4 printed wiring board (PWB. thickness: 1.6mm, Cu electrode surface: without surface coating). During the reflow soldering, the

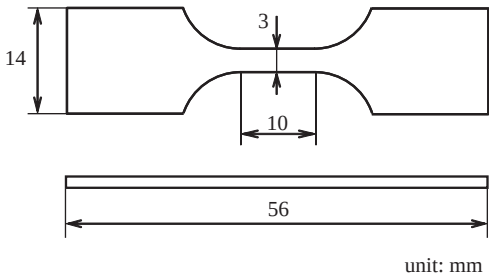

Fig. 1 Schematic illustration of the tensile test specimen.

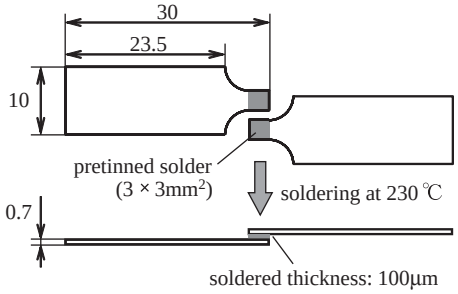

Fig. 2 Schematic illustration of the shearing test specimen.

sample was heated at a temperature higher than the solidus temperature for 30s, and up to the temperature 40°C to 45°C higher than the liquidus temperature. The thermal cycle test conditions employed were from -30°C to 80°C (the specimens were held at each temperature for 30 min) up to 3000 cycles, and -40°C to 125°C (30 min each) up to 1000 cycles.

In addition, Cu content in the solder joints was analyzed by EPMA (electron probe microanalysis) using the specimens for the thermal fatigue test to examine the amount of Cu leached from the Cu electrode on PWB into the solder.

2. 3 Characterization

Microstructures of the solder alloy and solder joint were analyzed by an optical microscope, SEM (scanning electron microscopy) and EPMA. The constituent phases in the solder alloy were identified by XRD (X-ray diffractometry).

3. Results and discussion

3. 1 Mechanical properties at 25°C

Tensile properties of Sn-Bi alloys and the influence of the addition of Cu on them were investigated. **Figure 3** shows appearances of the Sn-40Bi-0.1Cu and Sn-37Pb, before and after tensile tests, conducted at a strain rate of 1×10^{-4} s^{-1} and temperatures of 25°C and 80°C.

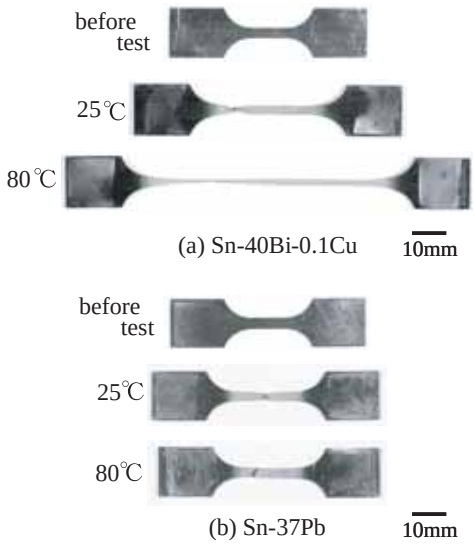

Fig. 3 Appearance of the specimen before and after the tensile test at 25°C and 80°C : (a) Sn-40Bi-0.1Cu and (b) Sn-37Pb.

Figure 4 shows the tensile properties of Sn-Bi alloys (Bi content: 0-62%). For comparison, the properties of 63%Sn-37%Pb (abbreviated as Sn-37Pb) were also shown.

The tensile strength increased with an increase in the Bi content up to approximately 10%, so that the tensile strength of Sn-10Bi (σ : 76MPa) became seven times as large as pure Sn (σ : 11MPa). Although the tensile strength decreases gradually with an increase in the Bi content over 10%, the tensile strengths of the alloys containing 40% to 62%Bi are still approximately five times as large as that of pure Sn.

On the other hand, elongation decreases rapidly with an increase in the Bi content up to 10%. Above that Bi content, however, the elongation increases with an increase in the Bi content and reaches the maximum value, 100-120%, between 30%Bi and 45%Bi, which are three to four times as large as that of pure Sn.

Figure 4 shows that low ductility, which has been known as a disadvantage of Bi-containing tin-based alloys caused by the solid solution hardening effect,[4] can be avoided if the Bi content is 30 to 45%. We previously reported that, by increasing the Bi content to 40% or more, fillet-lifting, another

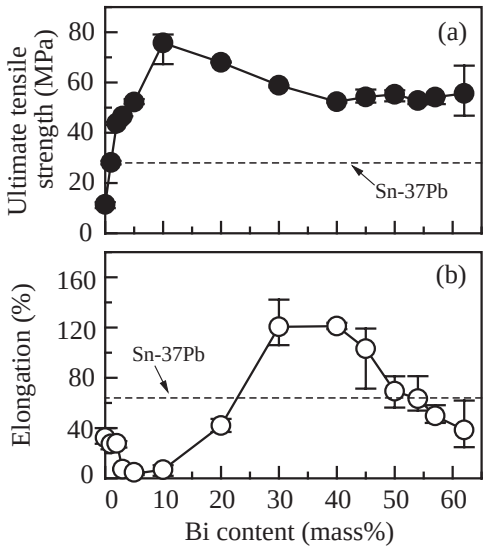

Fig. 4 Influence of Bi content on tensile properties of Sn-Bi alloys at 25°C : (a) ultimate tensile strength and (b) elongation. ---- : Sn-37Pb. The tensile strength and elongation were measured as the ultimate tensile strength and the total elongation to failure, respectively.

critical issue in bismuth-containing alloys,[7] can be restrained as shown in **Fig. 5**. Consequently, the optimal Bi content in the mechanical point of view in Sn-Bi alloy is 40 to 45%.

Figure 6 shows the influence of Cu content on the tensile properties of Sn-40Bi-Cu alloys. For comparison, the properties of Sn-37Pb were also shown. The tensile strength increases gradually as the copper content increases. In contrast, the elongation reaches the maximum value at 0.1%Cu, and subsequently decreases as the copper content increases. The elongation of the alloy containing 0.1%Cu is 171%, which is 1.4 times that of the alloy without Cu.

These results exhibited that tensile properties of Sn-Bi based alloy can surpass those of Sn-37Pb (σ : 28MPa, elongation: 64%) by the optimization of Bi content and the addition of Cu. The Sn-40Bi-0.1Cu, which is the optimum composition, has double the tensile strength (σ : 53MPa) and 2.5 times the elongation (elongation:171%) of Sn-37Pb. In addition, the addition of Cu does not affect the restraining effect for fillet-lifting of Sn-Bi alloy.

Figure 7 shows the relationship between the tensile properties and strain rate for Sn-40Bi-0.1Cu, at a strain rate of 1×10^{-4} to 1×10^{-2} s^{-1} and 25°C. For comparison, in Fig. 7, those for Sn-37Pb, Sn-57Bi which is typical low-melting lead-free solder, and Sn-57Bi-1Ag in which Ag is added to improve the ductility of Sn-57Bi[8, 9] are shown.

As shown in Fig. 7, for all the low-melting solders, the tensile strength increases and the elongation decreases as the strain rate increases. On the other hand, for Sn-37Pb, the tensile strength increases as the strain rate increases, while there is no remarkable change in the elongations as the strain rate change.

At the stain rate of 1×10^{-3} s^{-1} and below, which corresponds to the strain rate under thermal fatigue, the elongation of Sn-40Bi-0.1Cu is larger than that of Sn-37Pb. Sn-57Bi-1Ag has a larger ductility than Sn-37Pb at a strain rate of 1×10^{-4} s^{-1}, while its elongation is smaller than Sn-37Pb at a strain rate of

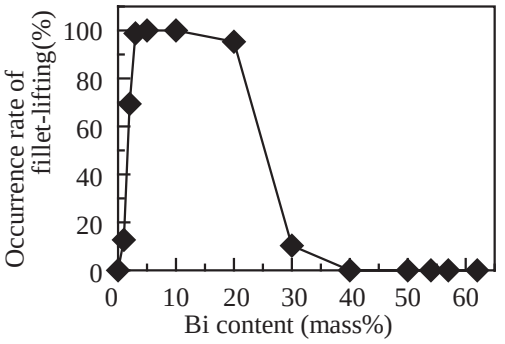

Fig. 5 Relationship between Bi content and the fillet-lifting occurrence rate in Sn-Bi alloys.[6]

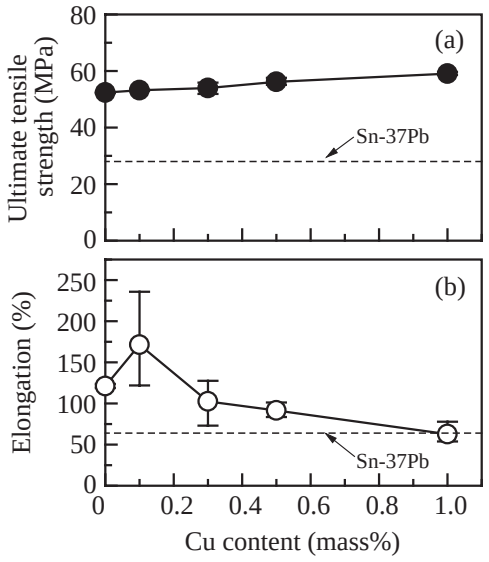

Fig. 6 Influence of Cu content on tensile properties of Sn-40Bi-Cu alloy at 25°C : (a) ultimate tensile strength and (b) elongation. ---- : Sn-37Pb

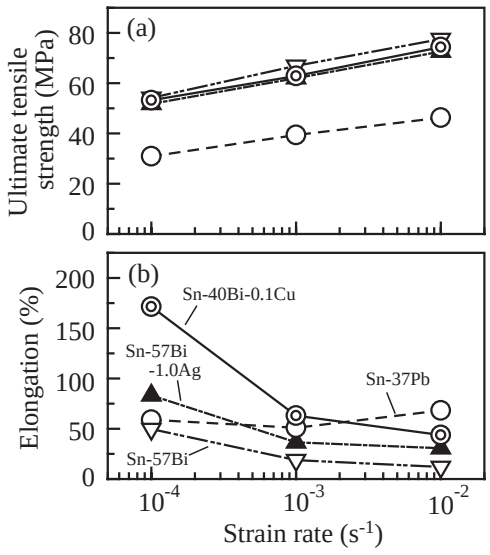

Fig. 7 Influence of strain rate on tensile properties of the alloys at 25°C : (a) ultimate tensile strength and (b) elongation. ◎ : Sn-40Bi-0.1Cu, ▲ : Sn-57Bi-1.0Ag, ▽ : Sn-57Bi and ○ : Sn-37Pb

1×10^{-3} s^{-1} and more.

3. 2 Mechanical properties at 80°C

As shown in Fig. 3 at 80°C, the elongation of Sn-40Bi-Cu alloys reaches above 500%, which is three times of that at 25°C and 10 times of that of Sn-37Pb (elongation: 54%) at 80°C, although the tensile strength of Sn-40Bi-0.1Cu (σ : 17MPa) at 80°C is smaller than that at 25°C, and close to that of Sn-37Pb (σ : 16MPa). These results show that the Sn-40Bi-Cu alloys have super plasticity at the high temperature, which have been reported for the extruded Sn-57Bi eutectic alloy[10] but not for the casted material.

3. 3 Mechanism of tensile deformation

Figures 8 shows the microstructure of Sn-40Bi and Sn-40Bi-0.1Cu before tensile test. The Sn-40Bi (Fig. 8(a)) consists of a Sn phase (the white area) of several dozen microns in size and a network structured Sn-Bi coexistence phase (the gray area) surrounding the Sn phase. According to the Sn-Bi binary phase diagram,[11] which shows the solidification process in which Sn-Bi eutectics crystallize after the primary crystallization of Sn, the large Sn phase is the primary crystallized Sn, and the network of Sn-Bi coexistence phase is Sn-Bi eutectics.

While Sn-40Bi-0.1Cu (Fig. 8(b)) has a similar structure with Sn-40Bi (Fig. 8(a)), the added Cu, as shown in **Fig. 9**, distributes mainly as fine particles of submicron in size and partly as particles of a few microns in size in the Sn-Bi eutectics. Both the Cu-containing particles were identified as Cu_6Sn_5 by XRD. Thus, the Cu_6Sn_5 particle forms a ternary eutectic phase in the Sn-40Bi-0.1Cu, as suggested from the facts that both Sn-Bi and Sn-Cu are eutectic systems (eutectic composition: Sn-57Bi and Sn-0.7Cu).[11]

Figure 10 shows the microstructure of the Sn-

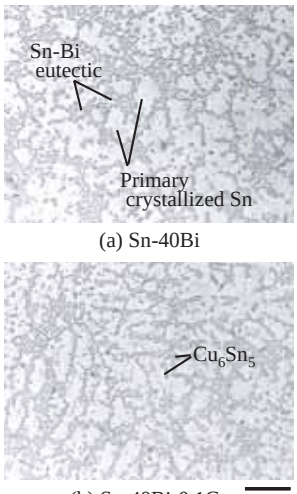

Fig. 8 Optical micrographs of the tensile test specimens before the test : (a) Sn-40Bi and (b) Sn-40Bi-0.1Cu.

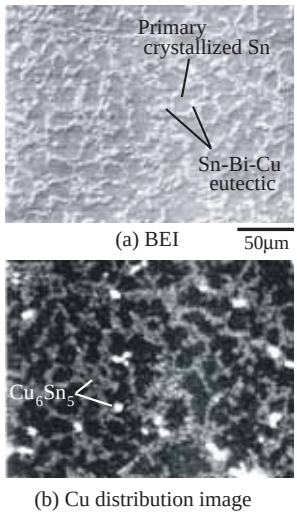

Fig. 9 Microstructure of Sn-40Bi-0.1Cu: (a) BEI (backscattered electron image) and (b) Cu distribution image by EPMA.

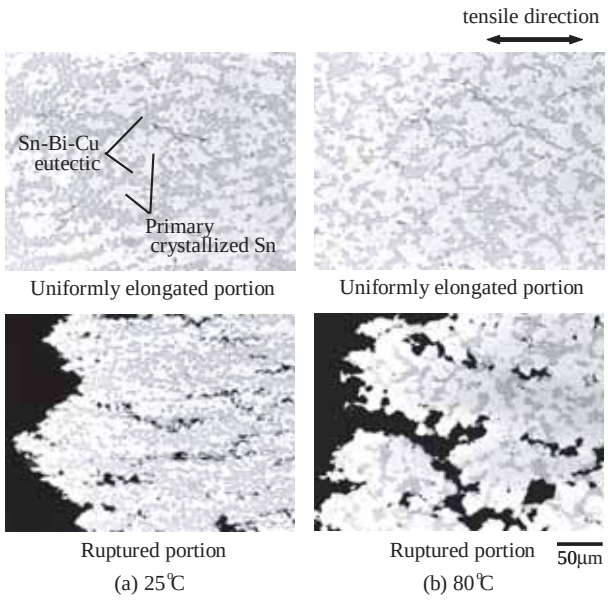

Fig. 10 Optical micrographs of the tensile test specimens after the test for Sn-40Bi-0.1Cu: (a) 25°C and (b) 80°C. upper: uniformly elongated and below: ruptured portion. The microstructure of Sn-40Bi after tensile test was similar to Sn-40Bi-0.1Cu, and therefore is not shown.

40Bi-0.1Cu (optical micrographs) after tensile test. While the region with the uniform elongation (the upper in Fig. 10(a)) preserves its original microstructure after the tensile test, in the ruptured portion (the bottom in Fig. 10(a)) at 25°C, a microstructure extends along the tensile direction due to necking. On the other hand, in the specimen tested at 80°C (Fig. 10(b). elongation: 516%), even in the ruptured portion, the original microstructure is preserved.

Figure 11 shows a schematic illustration of the two modes of deformation: grain change mode and grain boundary sliding mode.[12] It is known that, the polycrystalline materials usually deform with the first mode as shown in Fig. 11(b), in which the crystal grains elongates along the tensile direction without changing the geometry between adjacent grains. In some cases, however, deformation occurs with the second mode, in which sliding occurs at grain boundaries without deformation of crystal grains as shown in Fig. 11(c). In this case, super plastic deformation is known to occur.

The microstructure observation in Fig. 10 clearly shows that the super plastic behavior of Sn-Bi and Sn-Bi-Cu alloys is induced by this mechanism; the deformation occurs by sliding between the primary crystallized Sn phase and the Sn-Bi or Sn-Bi-Cu eutectic phase. This deformation mechanism can be rationally elucidated by the mechanical properties of these two phases. The primary crystallized Sn phase is unlikely to deform due to the solid solution hardening effect by Bi (Sn-10Bi tensile strength: 75 MPa, elongation: 7%). In contrast, the Sn-Bi and Sn-Bi-Cu eutectics (Sn-57Bi tensile strength: 54 MPa, elongation: 50%) can deform easily.

The super plasticity due to grain boundary sliding has been known only in a microstructure consisting of fine crystal grains of less than a few microns.[12] The super plasticity in the Sn-57Bi eutectic alloy[10] mentioned above is also due to a fine microstructure formed by the extrusion. In this study, however, it should be noted that the super plasticity arises even in a microstructure constructing of large crystal grains on the order of tens of microns.

Besides, the improvement in ductility by the addition of trace amounts of copper is likely to result from the fine distribution of Cu_6Sn_5 particles in the Sn-Bi-Cu eutectic phase.

3. 3 Reliability of solder joints

Figure 12 shows the shear strength for the lap-joint test specimens joined with Sn-40Bi-0.1Cu and Sn-37Pb solders. The strength of as-soldered Sn-40Bi-0.1Cu joint (initial strength) is 36MPa at 25°C and 19MPa at 80°C. Even after the heat treatment (80°C, 1000h), the strength is the same as that of as-soldered joint at either test temperature. In contrast, the strength of as-soldered Sn-37Pb joint (initial strength) considerably decreases after the heat treatment.

From these results, it is safely concluded that the shear strength of the Sn-40Bi-0.1Cu solder joint is always, at 25°C and 80°C, initially or after the heat treatment, higher than that of the Sn-37Pb solder joint.

Figures 13 show the optical micrographs of solder joint cross-sections, before and after the thermal

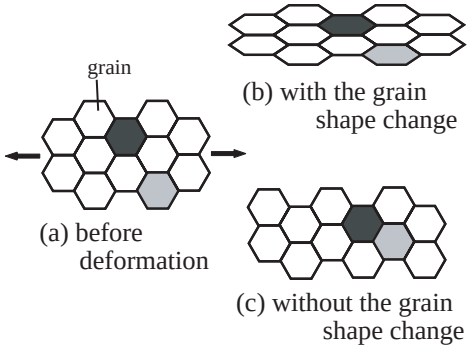

Fig. 11 Schematic illustration of the mode of grain boundary sliding in the tensile deformation: (a) before deformation, (b) and (c) after deformation.

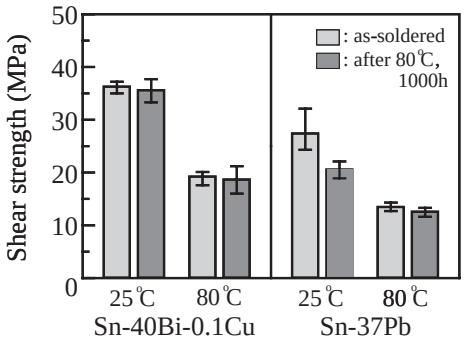

Fig. 12 Influence of the annealing at 80°C on the shear strength of Sn-40Bi-0.1Cu and Sn-37Pb solder joints at 25 and 80°C.

cycling test (-30°C to 80°C, 3000 cycles), for the resistors that were mounted using Sn-40Bi-0.1Cu and Sn-37Pb. The crack propagation ratio which is defined as 100% when a crack penetrates a solder joint thoroughly is additionally written in Fig. 13.

In the Sn-40Bi-0.1Cu joints after the thermal cycling test between -30°C and 80°C, as shown in Fig. 13(a), only a few small cracks are observed underneath and on the top of the resistor. The average crack propagation ratio is 3.5%, and its maximum value is 5%. In contrast, in the Sn-37Pb solder joint, as shown in Fig. 13(b), large cracks are clearly observed underneath and in the upper part of the resistor, and the crack propagation ratio reaches 50% or higher (average value: 64%).

Figure 14 shows the optical micrographs of the Sn-40Bi-0.1Cu solder joint cross-section after the 1000 cycles larger-temperature-range thermal cycling test between -40°C and 125°C. Although the surface of solder joint after the test became wholly rugged and the microstructure is coarsened, no crack is observed. In the Sn-37Pb joints, contrarily, the average crack propagation ratio reaches 44% under the same condition.

The reason that no crack occurred in the Sn-40Bi-0.1Cu joints is thought that the ductility of the alloy was further increased during the tests because the upper temperature, 125°C, was close to the solidus temperature (138°C) of Sn-40Bi-0.1Cu.

Table 1 shows the Cu content in the Sn-40Bi-0.1Cu and Sn-37Pb solder joint and thier increases from the original solder. The increase, which must be the leached Cu content from the PWB electrode into the molten solder, is significantly lower in the case of Sn-40Bi-0.1Cu than Sn-37Pb. This result shows that Sn-40Bi-0.1Cu restrains the dissolution of Cu during soldering.

4. Summary

We investigated the improvement effects of alloying in Sn-Bi on the mechanical properties and joint reliability. The following conclusions are derived from the present study.

(1) Optimization of the composition of Sn-Bi-Cu alloys, can improve the ductility and restrain fillet-lifting, simultaneously.

(2) Sn-Bi and Sn-Bi-Cu alloys containing about 40%Bi have super plasticity. The elongations of Sn-40Bi-0.1Cu are 171% at 25°C and 516% at 80°C, which are more than 2.5 times the ductility of the conventional Sn-37Pb solder alloy.

Table 1 Cu content and leached-Cu content from PWB.

Alloy composition	Cu content in the as-soldered joints	Leached-Cu content from PWB
Sn-40Bi-0.1Cu	0.19	0.09
Sn-37Pb	0.48	0.48

(mass%)

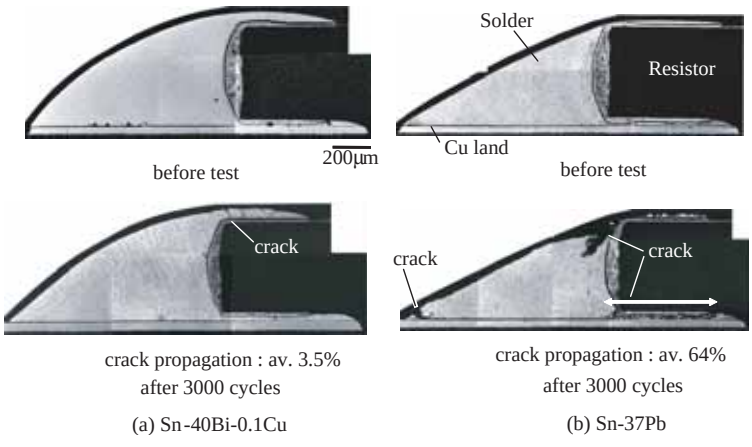

Fig. 13 Optical micrographs of the solder joint cross section for 4532 resistors before and after the thermal cycling test to 3000 cycles at -30 to 80°C : (a) Sn-40Bi-0.1Cu and (b) Sn-37Pb.
upper side: before the test, bottom side: after the test.

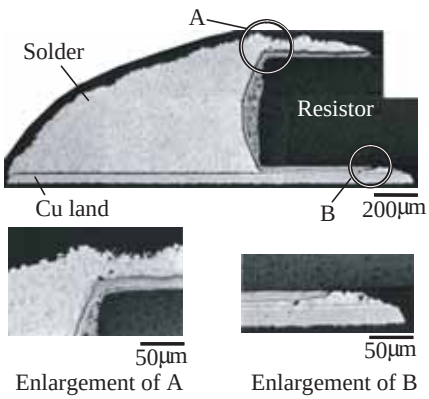

Fig. 14 Optical micrographs of the Sn-40Bi-0.1Cu solder joint cross section for 4532 resistor after the thermal cycling test to 1000 cycles at -40 to 125°C.

(3) The super plasticity in Sn-Bi and Sn-Bi-Cu alloys is attributed to the sliding between the primary crystallzed Sn phase and the Sn-Bi or Sn-Bi-Cu eutectic phase surrounding the Sn phase.

(4) The joint strength, the thermal fatigue resistance, and the Cu leaching resistance of soldered joints using Sn-40Bi-0.1Cu alloy are superior to those using Sn-37Pb alloy.

Table 2 shows the summary of the soldering properties of the newly developed Sn-40Bi-0.1Cu, compared to those of the conventional Sn-37Pb.

Table 2 Properties of Sn-40Bi-0.1Cu and Sn-37Pb.

Soldering property		Solder Alloy	
		Sn-40Bi-0.1Cu	Sn-37Pb
Melting temperature (^{o}C)		138-170	183
Melting range (^{o}C)		32	0
Spreading factor (%)		84 (250^{o}C)	95 (250^{o}C)
Ultimate tensile strength (MPa)	25^{o}C	53	28
	80^{o}C	17	16
Elongation (%)	25^{o}C	171	64
	80^{o}C	516	54
Coefficient of linear expansion ($^{o}C^{-1}$ at 25-120^{o}C)		13.9×10^{-6}	26.5×10^{-6}
Fillet-lifting		not occurred	not occurred
Cu leaching resistance		◎	○
Thermal fatigue resistance	-30 to 80^{o}C, 3000 cycles	◎	○
	-40 to 125^{o}C, 1000 cycles	◎	○
Migration resistance		○	○

◎: Good and ○: Fair

Migration test : 85^{o}C, relative humidity 85%, condition 16V applied during 1000h

References

1) Proposal for a directive on waste electrical and electronic equipment (WEEE) and proposal for a directive on the restriction of the use of certain hazardous substances in electrical and electronic equipment (ROHS): COM(2000)347 final, Commission of the European Communities, Brussels, (2000), 79
2) Official J. of the European Union, **45**-C90E(2002), 12-18
3) Official J. of the European Union, **46**-L37(2003), 19-23
4) Takemoto, T., Takahashi, M., Matsunawa, A., Ninomiya, R. and Tai, H. : Quarterly J. Jpn. Welding Soc., **16**(1998), 87-92
5) Vincent, J. H. and Humpston, G. : GEC J. Res., **11**-2 (1994), 76-89
6) Takao, H., Yamada, A., Hasegawa, H. and Matsui, M. : J. Jpn. Inst. Electron. Pack., **5**(2002), 152-158
7) Takao, H. and Hasegawa, H. : J. Electron. Mater., **30**(2001), 513-520
8) Ueda, H., Ochiai, M., Yamagishi, Y., Kitazima, M. and Takei, N. : Proc. 2nd Symp. Microjoining and Assembly Technolgy in Electronics, (1996), 159-162
9) McCormack, M., Chen, H. S., Kammlott, G. W. and Jin, S. : J. Electron. Mater., **26**(1997), 954-958
10) Pearson, C. E. : J. Inst. Metals, **54**(1934), 111-124
11) Binary Alloy Phase Diagrams Second Edition Plus Updates, Ed. by Massalski T. B., et al., (1996), (CD-ROM), ASM Int.
12) "*Chousosei to Kinzokukakougijutsu*", (in Japanese), Ed. by Chousoseikenkyukai, (1980), 53, The Nikkan Kogyo Shinbun, LTD., Tokyo

(Report received on May 20, 2004)

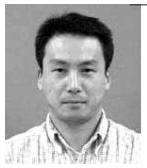

Hisaaki Takao
Year of birth : 1967
Division : Inorganic Materials Lab.
Research fields : Inorganic materials, Microelectronics technology
Academic degree : Dr. Eng.
Academic society : Jpn. Inst. Met., Jpn. Inst. Electron. Packaging
Awards : Paper Awards, MATE, 1999
R&D 100 Awards, 2003

Akira Yamada
Year of birth : 1951
Division : Metallic Materials Lab.
Research fields : Mechanical property of Metals and Inorganic materials
Awards : JSMS Award for Technical Developments, 1991

Hideo Hasegawa
Year of birth : 1942
Division : Metallic Materials Lab.
Research fields : Metals and Inorganic materials, Microelectronics technology
Academic degree : Dr. Eng.
Academic society : Jpn. Inst. Met., Ceram. Soc. Jpn.
Awards : Paper Awards, Jpn. Inst. of Metals, 1987,
Paper Awards, MATE, 1999
R&D 100 Awards, 2003